ORIGINAL PAPER

QSAR, DFT and quantum chemical studies on the inhibition potentials of some carbozones for the corrosion of mild steel in HCl

Nnabuk O. Eddy · Benedict I. Ita

Abstract Experimental aspects of the inhibition of the corrosion of mild steel in HCl solutions by some carbozones were studied using gravimetric, thermometric and gasometric methods, while a theoretical study was carried out using density functional theory, a quantitative structure–activity relation, and quantum chemical principles. The results obtained indicated that the studied carbozones are good adsorption inhibitors for the corrosion of mild steel in HCl. The inhibition efficiencies of the studied carbozones were found to increase with increasing concentration of the respective inhibitor. A strong correlation was found between the average inhibition efficiency and some quantum chemical parameters, and also between the experimental and theoretical inhibition efficiencies (obtained from the quantitative structure–activity relation).

Keywords Corrosion · Inhibition · Carbozones · Experimental and theoretical studies

Abbreviations

χ	Electronegativity
η	Global hardness
ΔE	Energy gap (i.e. $E_{LUMO} - E_{HOMO}$)
μ	Dipole moment
σ	Chemical potential
C–C	Core–core repulsion energy
Cosmo	Conductor-like screening model
CosA	Cosmo area
CosV	Cosmo volume
DFT	Density functional theory
EA	Electron affinity
EE	Electronic energy of a molecule
E_{HOMO}	Energy of the highest occupied molecular orbital
E_{LUMO}	Energy of the lowest unoccupied molecular orbital
$E_{(N-1)}$	Ground state energy of the system with N−1 electrons
$E_{(N)}$	Ground state energy of the system with N electrons
$E_{(N+1)}$	Ground state energy of the system with N+1 electrons
f^+	Fukui function for the nucleophile
f^-	Fukui function for the electrophile
S	Global softness
S^+	Global softness for the nucleophile
S^-	Global softness for the electrophile
IP	Ionization potential
q	Mulliken charge
Q_{ads}	Heat of adsorption
QSAR	Quantitative structure activity relation
R	Gas constant
TE	Total energy of the molecule
AM1	Austin model 1
PM3	Parametric method number 3
PM6	Parametric method number 6
RM1	Recife model
MNDO	Modified neglect of diatomic overlap

N. O. Eddy (✉)
Department of Chemistry, Ahmadu Bello University,
Zaria, Kaduna State, Nigeria
e-mail: nabukeddy@yahoo.com

B. I. Ita
Department of Chemistry, University of Calabar,
Calabar, Cross River State, Nigeria

Introduction

The corrosion of metals, including mild steel, is a serious problem in most industries, especially during processes such as pickling of steel, acid washing and etching [1–4]. Although several options are available for the protection of mild steel against corrosion, the use of organic inhibitors is one of the best options [5–12]. Most corrosion inhibitors are organic compounds that have electronegative functional groups and π-electrons in multiple bonds [13–15]. In most cases, the presence of heteroatoms such as N, S, O, P as well as aromatic ring(s) facilitates the adsorption of the inhibitor onto the metal surface, which is the initial mechanism for the inhibition process [16].

The quantum chemical principle is a great tool that can be used to predict the inhibition potentials of some organic compounds that are structurally related. This is because strong correlations have been found between the corrosion inhibition efficiencies of most compounds and some semiempirical parameters [17]. The use of density functional theory has also proven to be suitable for predicting sites of electrophilic and nucleophilic attack during the corrosion inhibition process [18]. In some cases, a quantitative structure–activity relation (QSAR) has been used to derive equations for the theoretical inhibition efficiency. The results obtained from such calculations can be of great help in the synthesis of new corrosion inhibitors [19]. The objective of the present study was to investigate the inhibition potentials of some carbozones using experimental and theoretical techniques. The investigated compounds are listed below, while their chemical and optimized structures are presented in Fig. 1

(a)   2-(Diphenylmethylene)-N-phenylhydrazinecarbothioamide (DPHCARB)

(b)   (E)-N-methyl-2-(1-phenylethylidene)hydrazinecarbothioamide (PHCARB)

(c)   (E)-2-(2-oxo-1,2-diphenylethylidene)-N-phenylhydrazinecarbothioamide (ODPPHCARB)

(e)   (E)-2-(2-hydroxy-1,2-diphenylethylidene)-N-phenyl-hydrazinecarbothioamide (HDPPCARB)

Experimental techniques

Materials

The material used for the study was a mild steel sheet of composition (wt%): Mn (0.6), P (0.36), C (0.15) and Si (0.03), and Fe (the rest). The sheet was mechanically pressed cut into different coupons, each of size $5 \times 4 \times 0.11$ cm. Each coupon was degreased by washing with ethanol, dipped in acetone, and allowed to dry in air before it was preserved in a desiccator. All reagents used for the study were Analar grade, and double-distilled water was used for their preparation.

The inhibitors were synthesized and supplied by Prof. E. E. Offiong of the Department of Chemistry, University of Calabar, Nigeria. The range of inhibitor concentrations used was 1×10^{-4} to 5×10^{-4} M. Each of these concentrations was dissolved in 0.1 M HCl (for use in gravimetric analysis) and in 2.5 M HCl (for use in gasometric and thermometric analysis), respectively.

Gravimetric method

In the gravimetric experiment, a previously weighed metal (mild steel) coupon was completely immersed in 250 ml of the test solution in an open beaker. The beaker was covered with aluminum foil and inserted into a water bath maintained at

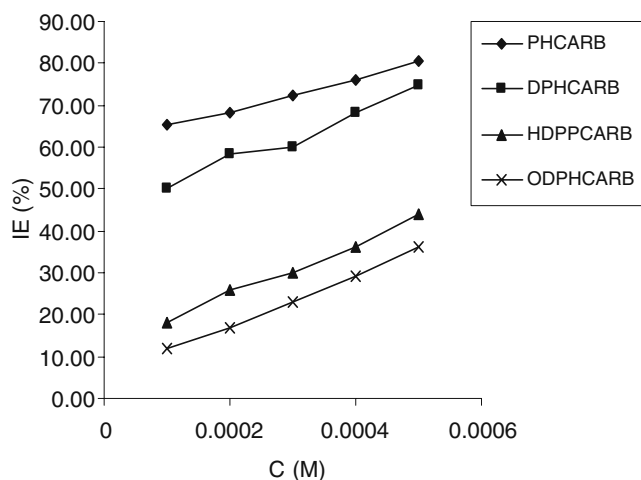Fig. 1 Chemical structures of the studied inhibitors
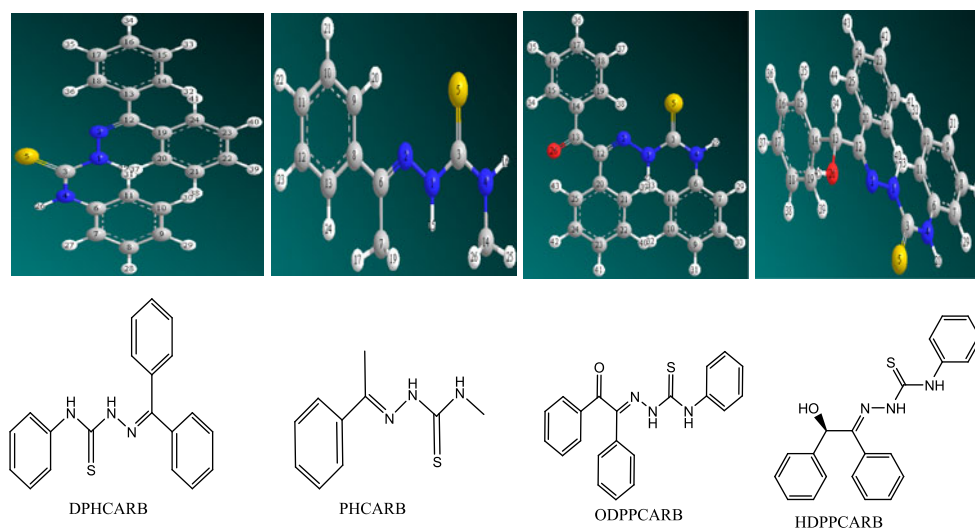
Fig. 2 Variations of the inhibition efficiencies of the studied inhibitors with concentration

303 K. Every 24 h, the corrosion product was removed by washing each coupon (withdrawn from the test solution) in a solution containing 50% NaOH and 100 g l^{-1} of zinc dust. The washed coupon was rinsed in acetone and dried in the air before it was re-weighed. The change in weight over a period of 168 h was taken as the total weight loss. From the average weight loss results (average of three replicate analyses), the inhibition efficiency (E_{exp}) of the inhibitor and the degree of surface coverage were calculated using Eqs. 1 and 2, respectively [20]:

$$IE_{exp} = (1 - W_1/W_2) \times 100 \tag{1}$$

$$\theta = 1 - W_1/W_2, \tag{2}$$

where W_1 and W_2 are the weight losses (g) for mild steel in the presence and absence of the inhibitor, and θ is the degree of surface coverage of the inhibitor.

Gasometric method

Gasometric methods were carried out at 303 K as described in the literature [21]. From the volume of hydrogen gas evolved per minute, inhibition efficiencies were calculated using Eq. 3:

$$IE_{exp} = \left(1 - \frac{V_{Ht}^1}{V_{Ht}^o}\right) \times 100, \tag{3}$$

where V_{Ht}^1 and V_{Ht}^o are the volumes of H$_2$ gas evolved at time t for inhibited and uninhibited solutions, respectively.

Thermometric method

This was also carried out as reported elsewhere [22]. From the rise in temperature of the system per minute, the reaction number (RN) was calculated using Eq. 4:

$$RN\left(^\circ C\ min^{-1}\right) = \frac{T_m - T_i}{t}, \tag{4}$$

where T_m and T_i are the maximum and initial temperatures, respectively, and t is the time (min) taken to reach the maximum temperature. The inhibition efficiency (IE_{exp}) of the inhibitor was evaluated from the percentage reduction in the reaction number as follows:

$$IE_{exp} = \left(RN_{aq} - RN_{wt}\right)/RN_{aq} \times 100, \tag{5}$$

Table 1 Inhibition efficiencies of the studied inhibitors

| Method	Inhibition efficiency (%)	C×10^{-4} (M)				
		1	2	3	4	5
Gravimetric	PHCARB at 303 K	65.23	68.24	72.15	76.23	80.68
	PHCARB at 333 K	58.23	60.15	64.21	68.15	72.77
	DPHCARB at 303 K	50.23	58.45	60.00	68.11	74.59
	DPHCARB at 333 K	32.32	38.11	44.21	50.12	52.95
	HDPPCARB at 303 K	18.01	26.04	30.00	36.00	44.02
	HDPPCARB at 333 K	24.00	30.32	36.10	48.00	60.01
	ODPPCARB at 303 K	12.12	17.00	23.01	29.00	36.01
	ODPPCARB at 333 K	26.03	32.02	40.04	47.01	55.00
Gasometric	PHCARB at 303 K	62.11	67.84	70.02	77.89	82.93
	DPHCARB at 303 K	50.56	62.34	65.02	70.20	72.34
	HDPPCARB at 303 K	52.32	60.01	71.02	78.99	83.45
	ODPPCARB at 303 K	50.23	59.76	63.43	74.05	78.99
Thermometric	PHCARB at 303 K	64.87	68.04	71.24	79.34	84.23
	HDPPCARB at 303 K	53.21	57.89	62.01	72.34	76.33
	ODPPCARB at 303 K	52.23	54.87	61.08	71.98	78.88
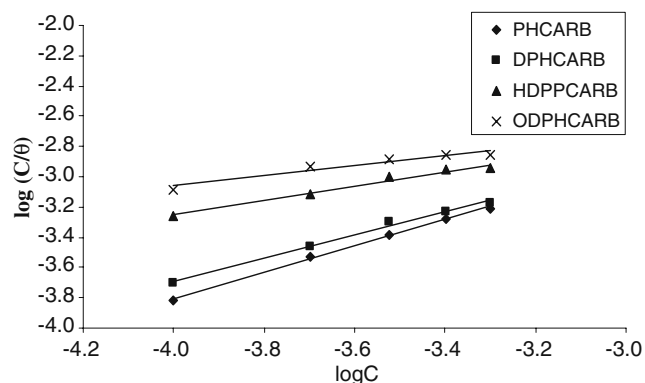
Fig. 3 Langmuir isotherms for the adsorption of the studied inhibitors on the mild steel surface at 303 K

where RN_{aq} is the reaction number in the absence of inhibitors (blank solution) and RN_{wi} is the reaction number of the H_2SO_4 containing the inhibitors.

Quantum chemical calculations

Single point energy calculations were carried out using the AM1, PM6, PM3, MNDO and RM1 Hamiltonians in the software package MOPAC 2008 for Windows. Calculations were performed on an HP Pentium V (3.0 GHz, 3 GB RAM and 300 GB hard disc) computer. The following

quantum chemical indices were calculated: the energy of the highest occupied molecular orbital (E_{HOMO}), the energy of the lowest unoccupied molecular orbital (E_{LUMO}), the dipole moment (μ), the total energy (TE), the electronic energy (EE), the ionization potential (IP), the Cosmo area (CosA), and the Cosmo volume (CosV). The Mulliken and Löwdin charges (q) on the atoms were computed using the GAMES computational software. The correlation type and method used for the calculation was MP2, while the basis set was STO-3G.

Statistical analyses were performed using SPSS version 15.0 for Windows. Nonlinear regression analyses were performed using an unconstrained sum of squared residuals for the loss function and the estimation methods of Levenberg–Marquardt in SPSS version 15.0 for Windows.

Results and discussion

Experimental study

Figure 2 shows the variations in the inhibition efficiencies of PHCARB, HDPPCARB and ODPPCARB with concentration at 303 K. The figure reveals that the inhibition efficiencies of these inhibitors increase with increasing concentration, which indicates that the inhibitors are

Table 2 Quantum chemical parameters for the studied inhibitors

|	Models	E_{HOMO} (eV)	E_{LUMO} (eV)	ΔE (eV)	EE (eV)	C–C (eV)	CosA (Å^2)	CosV (Å^3)	μ (Debye)
PHCARB	PM6	−8.600	−0.682	7.918	−12965.01	10853.79	240.03	246.48	5.988
	PM3	−8.630	−0.900	7.730	−12662.38	10608.58	240.03	246.48	2.568
	AMI	−8.532	−0.553	7.979	−13048.31	10777.91	240.03	246.48	2.710
	RMI	−8.681	−0.447	8.234	−13116.67	10865.21	240.03	246.48	2.857
	MNDO	−8.680	−0.666	8.014	−13110.94	10802.66	240.03	246.48	3.522
HDPPCARB	PM6	−7.573	−0.933	6.640	−34944.10	30829.62	364.88	418.50	2.270
	PM3	−7.221	−0.944	6.277	−34389.41	30360.23	364.88	418.50	3.540
	AMI	−7.059	−0.566	6.493	−35096.82	30702.68	364.88	418.50	3.706
	RMI	−7.497	−0.539	6.958	−35228.29	30888.66	364.88	418.50	3.635
	MNDO	−7.236	−0.727	6.509	−35184.03	30750.40	364.88	418.50	4.731
ODPPCARB	PM6	−6.981	−2.615	4.366	−31720.63	27944.88	341.05	382.10	4.410
	PM3	−7.464	−1.712	5.752	−31108.42	27415.17	341.05	382.10	5.260
	AMI	−7.215	−1.438	5.777	−31799.09	27766.02	341.05	382.10	4.920
	RMI	−7.624	−1.364	6.260	−31945.14	27961.71	341.05	382.10	5.288
	MNDO	−7.304	−1.456	5.848	−31881.76	27813.51	341.05	382.10	5.091
DPHCARB	PM6	−8.587	−1.136	7.451	−28887.97	25648.07	310.91	348.13	6.069
	PM3	−8.581	−1.331	7.250	−28223.61	24981.00	310.91	348.13	6.818
	AMI	−8.317	−0.867	7.450	−28856.07	25310.26	310.91	348.13	6.373
	RMI	−8.450	−0.779	7.671	−29026.11	25523.46	310.91	348.13	6.734
	MNDO	−8.378	−0.791	7.587	−28933.03	25358.03	310.91	348.13	6.193
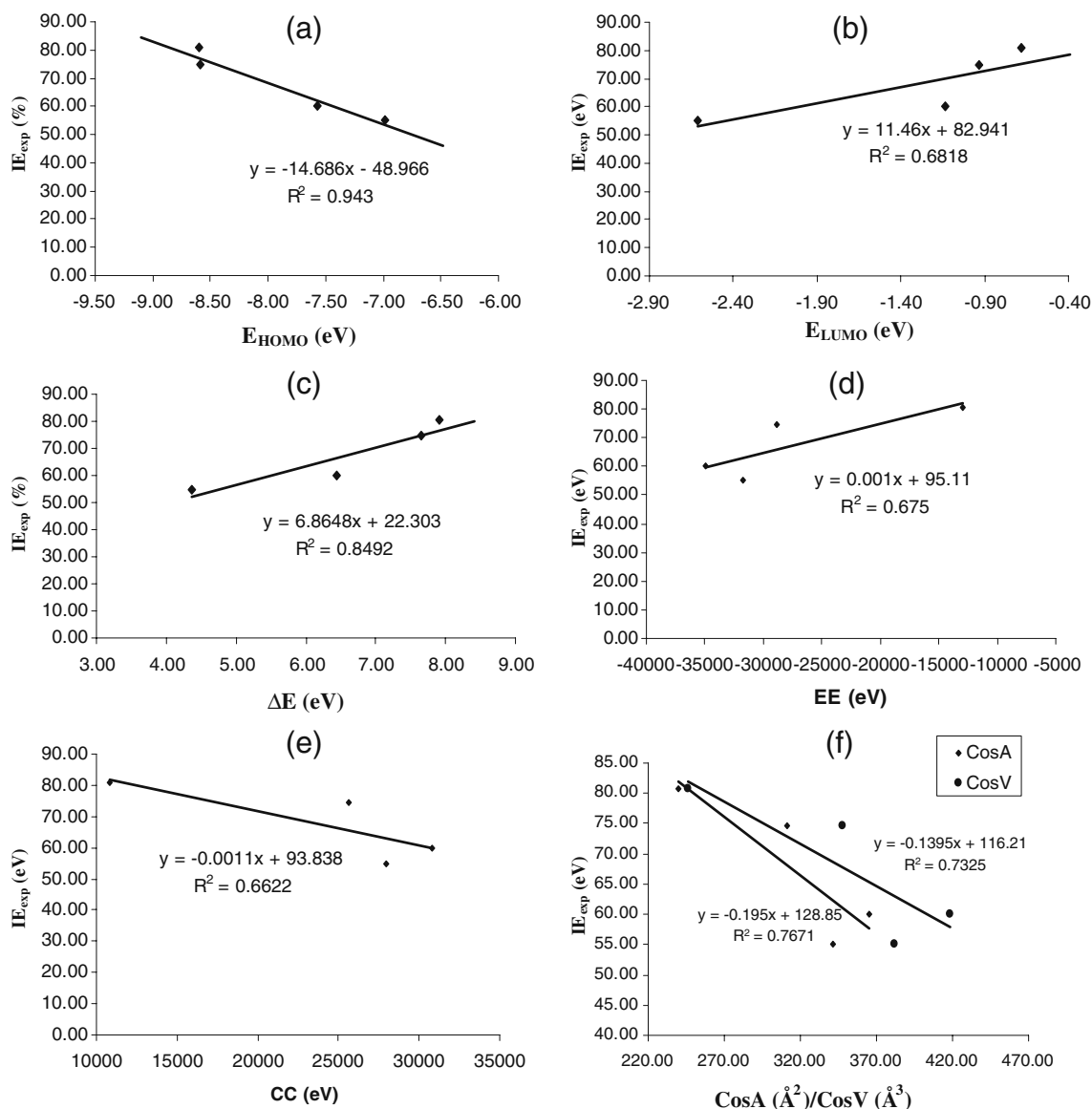
Fig. 4 Variations of the experimental inhibition efficiencies (IE$_{exp}$) of the studied carbozones with E_{HOMO}, ΔE, EE, C–C, CosA and CosV

adsorption inhibitors for the corrosion of mild steel in HCl solutions. The inhibition efficiencies of the studied inhibitors are presented in Table 1. The results obtained indicate that the inhibition efficiencies of the inhibitors increase with increasing concentration and with increasing temperature (except for PHCARB and DPHCARB). This also implies that HDPPCARB and ODPPCARB are adsorbed on the surface of mild steel through the mechanism of chemical adsorption, while the adsorption of PHCARB and DPHCARB on mild steel surface supports the mechanism of physical adsorption. For a physical adsorption mechanism, the inhibition efficiency of the inhibitor will decrease with increasing temperature; for a chemical adsorption mechanism, the inhibition efficiency increases with increasing temperature [23].

Values of inhibition efficiencies obtained from the gasometric and thermometric methods are also presented in Table 1. From the results obtained, the inhibition efficiencies obtained from the thermometric and gasometric methods are higher than those obtained from the gravimetric method. This indicates that the instantaneous inhibition efficiencies of the studied inhibitors are better than their average inhibition efficiencies, because gravimetric analysis measures the average inhibition efficiency, while gasometric and thermometric methods measure the instantaneous inhibition efficiencies of an inhibitor.

The adsorption characteristics of the inhibitors were studied by fitting the data obtained for the degree of surface coverage to different adsorption isotherms. The tests revealed that the isotherm that best describes the adsorption

behavior of the inhibitors is the Langmuir isotherm, which can be expressed as follows [24]:

$$\log(C/\theta) = \log C - \log K_{ads}, \tag{6}$$

where C is the concentration of the inhibitor in the bulk electrolyte, θ is the degree of surface coverage of the inhibitor, and K_{ads} is the equilibrium constant of adsorption. Using Eq. 6, the plots of $\log(C/\theta)$ versus $\log C$ (Fig. 3) were linear (R^2 values ranged from 0.9288 to 0.9943), confirming the applicability of the Langmuir adsorption model to the adsorption of the inhibitors on the mild steel surface. At 313 K, the adsorption characteristics of the inhibitors were also consistent with the Langmuir adsorption model (plot not shown). However, R^2 values for the plots were found to range from 0.893 to 0.9971.

The equilibrium constant of adsorption expressed in Eq. 6 is related to the free energy of adsorption as follows [25]:

$$\Delta G^0_{ads} = -2.303RT\log(55.5K), \tag{7}$$

where K is the equilibrium constant of adsorption, 55.5 is the molar concentration of water, $\Delta G_{ads}{}^0$ is the free energy of adsorption of the inhibitor, R is the gas constant, and T is the temperature. The free energies of adsorption (at 303 K) calculated from Eq. 7 were −20.23, −13.68, −18.01 and −11.96 kJ mol^{-1} for ODPPCARB,

DPHCARB, HDPPCARB, and PHCARB, respectively. These results are consistent with the mechanism of physical adsorption and indicate that the adsorption of the inhibitors on the mild steel surface is spontaneous. It is also worth noting that the occurrence of a physical adsorption process does not in any way stop a chemical adsorption process from occurring. However, prior to chemical adsorption, there must be physical adsorption [26].

Quantum chemical study

Table 2 presents values of quantum chemical parameters (calculated for the PM6, PM3, AM1, RM1 and MNDO Hamiltonians) for PHCARB, HDPPCARB, ODPP-CARB, and DPHCARB. From the results obtained, it is evident that the average experimental inhibition efficiencies of the inhibitors increase with increasing energy of the highest occupied molecular orbital (E_{HOMO}), but decrease with increasing energy of the lowest unoccupied molecular orbital (E_{LUMO}), and also with the energy gap ($\Delta E = E_{HOMO} - E_{LUMO}$). E_{HOMO} and E_{LUMO} are the energies of the frontier molecular orbitals, and they can be used to predict the reactivity of an organic molecule. According to frontier molecular orbital theory, the formation of a transition state can be viewed in terms of the interaction between the frontier molecular

Table 3 Quantum chemical descriptors for the studied inhibitors

|	Model	E_N (eV)	E_{N-1} (eV)	E_{N+1} (eV)	IE (eV)	EA (eV)	χ (eV)	S (/eV)	η (eV)	δ
PHCARB	PM6	−2111.22	−2103.27	−2112.63	7.95	1.41	4.68	0.15	6.54	0.18
	PM3	−2053.8	−2045.75	−2054.12	8.05	0.32	4.18	0.13	7.73	0.18
	AM1	−2270.41	−2262.42	−2270.46	7.99	0.05	4.02	0.13	7.94	0.19
	RM1	−2251.46	−2243.52	−2251.82	7.94	0.36	4.15	0.13	7.58	0.19
	MNDO	−2308.29	−2300.36	−2309.69	7.93	1.40	4.67	0.15	6.53	0.18
HDPPCARB	PM6	−4114.48	−4108.49	−4116.37	5.99	1.89	3.94	0.24	4.10	0.37
	PM3	−4029.17	−4022.90	−4030.87	6.27	1.70	3.98	0.22	4.57	0.33
	AM1	−4394.14	−4388.11	−4394.60	6.03	0.46	3.25	0.18	5.57	0.34
	RM1	−4339.63	−4333.16	−4341.05	6.47	1.42	3.95	0.20	5.05	0.30
	MNDO	−4433.63	−4427.52	−4435.13	6.11	1.50	3.80	0.22	4.61	0.35
ODPPCARB	PM6	−3775.75	−3771.97	−3780.70	5.95	3.78	4.87	0.46	2.17	0.49
	PM3	−3693.24	−3686.80	−3694.64	6.44	1.40	3.92	0.20	5.04	0.31
	AM1	−4033.07	−4026.96	−4035.38	6.11	2.31	4.21	0.26	3.80	0.37
	RM1	−3983.43	−3976.91	−3985.72	6.52	2.29	4.40	0.24	4.23	0.31
	MNDO	−4068.24	−4062.15	−4070.58	6.09	2.34	4.21	0.27	3.75	0.37
DPHCARB	PM6	−3239.90	−3231.76	−3239.95	8.14	0.05	4.10	0.124	8.09	0.18
	PM3	−3242.61	−3233.51	−3244.20	9.10	1.59	5.35	0.133	7.51	0.11
	AM1	−3545.81	−3537.38	−3546.53	8.43	0.72	4.58	0.130	7.71	0.16
	RM1	−3502.65	−3494.20	−3504.19	8.45	1.54	5.00	0.145	6.91	0.15
	MNDO	−3575.00	−3566.63	−3576.60	8.37	1.6	4.99	0.148	6.77	0.15
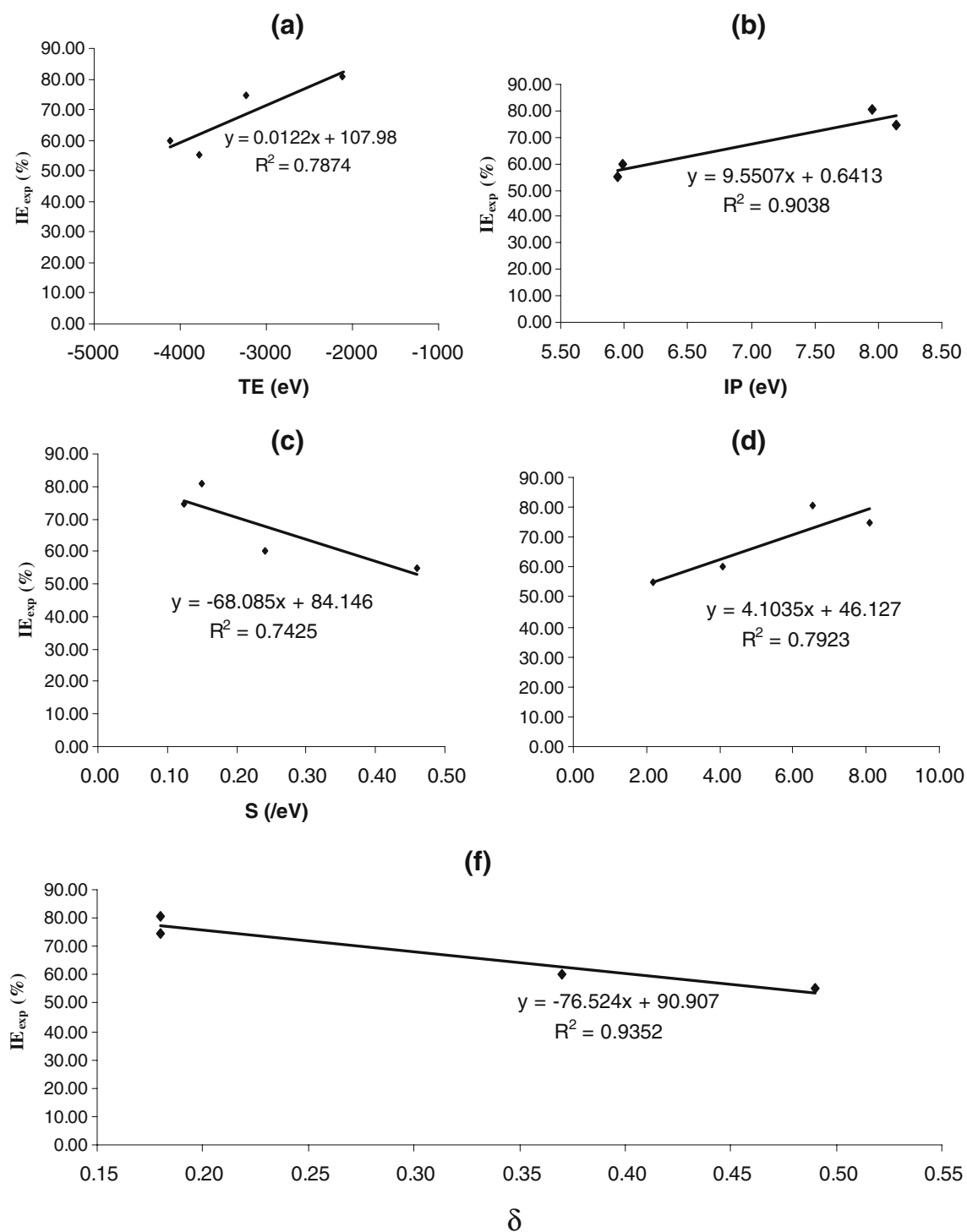
Fig. 5 Variations of the experimental inhibition efficiencies (IE$_{exp}$) of the studied carbozones with IE, EA, S and δ

orbitals (HOMO and LUMO) of the reactants [27–29]. E_{HOMO} indicates the ability of the molecule to donate an electron, while E_{LUMO} indicates the ability of the molecule to accept an electron. Therefore, increasing E_{HOMO} and decreasing E_{LUMO} indicates that the adsorption of the inhibitors on the mild steel surface is

facilitated by a donor–acceptor mechanism. On the other hand, the energy gap (ΔE) is an important stability index. A large ΔE implies high molecular stability in chemical reactions [30]. ΔE has also been associated with activation hardness and polarizability. Therefore, a decrease in the value of ΔE implies that the molecule is

Table 4 Fukui and global softness indices for nucleophilic and electrophilic attacks on PHCARB, calculated from Mulliken (Löwdin) charges (STO-3G)

Atom	f^+ (|e|)	f^- (|e|)	S^+ (eV|e|)	S^- (eV|e|)
N1	−8.1157 (−7.9202)	−0.0458 (0.0122)	−2.3535 (−2.2968)	−0.0133 (0.0035)
N2	0.0046 (0.0491)	**2.1832 (1.9348)**	0.0013 (0.0142)	0.6331 (0.5611)
C3	−7.9981 (−7.9980)	−0.0004 (0.0001)	−2.3195 (−2.3194)	−0.0001 (0.0000)
N4	−7.9968 (−7.9979)	0.0000 (0.0000)	−2.3191 (−2.3194)	0.0000 (0.0000)
S5	−8.0047 (−8.0022)	−0.0002 (0.0017)	−2.3214 (−2.3206)	0.0000 (0.0005)
C6	−7.9962 (−8.0005)	−0.0001 (0.0000)	−2.3189 (−2.3201)	0.0000 (0.0000)
C7	−7.9965 (−8.0005)	0.0000 (0.0000)	−2.3190 (−2.3201)	0.0000 (0.0000)
C8	−7.9962 (−8.0004)	0.0000 (0.0000)	−2.3189 (−2.3201)	0.0000 (0.0000)
C9	−7.9955 (−7.9998)	−0.0001 (0.0000)	−2.3187 (−2.3199)	0.0000 (0.0000)
C10	−7.9785 (−7.9833)	−0.0002 (0.0000)	−2.3138 (−2.3151)	−0.0001 (0.0000)
C11	−8.0153 (−7.9998)	0.0018 (0.0000)	−2.3244 (−2.3199)	0.0005 (0.0000)
C12	**8.0959 (7.8604)**	−0.1548 (0.0403)	2.3478 (2.2795)	−0.0449 (0.0117)
C13	8.0096 (7.9831)	−0.0002 (0.0007)	2.3228 (2.3151)	0.0000 (0.0002)
C14	8.0020 (**7.9839**)	0.0000 (0.0000)	2.3206 (2.3153)	0.0000 (0.0000)
C15	7.2061 (6.8647)	0.0000 (0.0000)	2.0898 (1.9908)	0.0000 (0.0000)
C16	2.7465 (2.9983)	0.0000 (0.0000)	0.7965 (0.8695)	0.0000 (0.0000)
C17	1.7562 (2.0310)	0.0000 (0.0000)	0.5093 (0.5890)	0.0000 (0.0000)
C18	7.2282 (6.7738)	−0.0003 (0.0001)	2.0962 (1.9644)	−0.0001 (0.0000)
C19	8.0356 (7.9370)	0.0758 (−0.0031)	2.3303 (2.3017)	0.0220 (−0.0009)
C20	4.4872 (4.0521)	−2.1537 (−2.0748)	1.3013 (1.1751)	−0.6246 (−0.6017)
C21	6.0311 (5.6171)	−1.0148 (−0.8886)	1.7490 (1.6289)	−0.2943 (−0.2577)
C22	7.9514 (7.9508)	0.0588 (−0.0062)	2.3059 (2.3057)	0.0171 (−0.0018)
C23	7.9960 (7.9999)	0.0000 (−0.0003)	2.3188 (2.3200)	0.0000 (−0.0001)
C24	7.9942 (7.9995)	−0.0004 (0.0000)	2.3183 (2.3199)	−0.0001 (0.0000)

soft and can be easily polarized. Therefore, the trend in the experimental inhibition efficiencies of the inhibitors (PHCARB>DPHCARB>>ODPPCARB>HDPPCARB) is consistent with the findings obtained from the frontier molecular orbitals of the inhibitors. Similar trends were also obtained with respect to the electronic energy (EE), the core–core repulsion energy (C–C), Cosmo area

(CosA), and Cosmo volume (CosV) of the inhibitors. Figure 4 presents plots showing the variations in the experimental inhibition efficiencies (IE$_{exp}$) of the inhibitors with some quantum chemical parameters calculated for the PM6 model. Plots for other models, and for parameters that had R^2 values less than 0.5, are not shown. However, it was observed that other Hamiltonians gave

Table 5 Fukui and global softness indices for nucleophilic and electrophilic attacks on PHCARB, calculated from Mulliken (Löwdin) charges (STO-3G)

Atom	f^+ (|e|)	f^- (|e|)	S^+ (eV|e|)	S^- (eV|e|)
C1	−0.051 (−0.069)	−0.019 (−0.027)	−0.007 (−0.010)	−0.003 (−0.004)
C2	−0.017 (−0.017)	−0.003 (−0.001)	−0.002 (−0.002)	0.000 (0.000)
C3	−0.038 (−0.047)	−0.013 (−0.016)	−0.005 (−0.006)	−0.002 (−0.002)
C4	−0.042 (−0.051)	0.016 (0.025)	−0.006 (−0.007)	0.002 (0.004)
C5	−0.040 (−0.049)	−0.017 (−0.021)	−0.006 (−0.007)	−0.002 (−0.003)
C6	−0.019 (−0.019)	−0.004 (−0.003)	−0.003 (−0.003)	−0.001 (0.000)
C7	−0.098 (−0.121)	−0.059 (−0.076)	−0.014 (−0.017)	−0.008 (−0.011)
C8	**0.006 (0.004)**	0.006 (0.004)	**0.001 (0.001)**	0.001 (0.001)
N9	−0.129 (−0.154)	**0.021 (0.037)**	−0.018 (−0.021)	**0.003 (0.005)**
N10	**0.004 (0.011)**	−0.040 (−0.049)	**0.001 (0.002)**	−0.006 (−0.007)
C11	−0.014 (−0.017)	−0.001 (0.005)	−0.002 (−0.002)	0.000 (0.001)
S12	−0.123 (−0.118)	−0.594 (−0.622)	−0.017 (−0.016)	−0.083 (−0.086)
N13	−0.013 (−0.015)	−0.040 (−0.052)	−0.002 (−0.002)	−0.006 (−0.007)
C14	0.002 (0.000)	**0.022 (0.014)**	0.000 (0.000)	**0.003 (0.002)**

results that are comparable to those obtained for the PM6 Hamiltonian. From Fig. 4, it can be seen that there is a strong correlation between the calculated quantum chemical parameters and the experimental inhibition efficiencies, indicating that these parameters are good indices for predicting the inhibition of mild steel corrosion by the studied carbozones.

The dipole moment (μ) is an index that can also be used for predicting the direction of a corrosion inhibition process. The dipole moment is a measure of the polarity of a covalent bond, and it is related to the distribution of electrons in a molecule [31]. Although literature is inconsistent on the use of μ as a predictor for the direction of a corrosion inhibition reaction, it is generally agreed that the adsorption of polar compounds possessing high dipole moments onto the metal surface should lead to better inhibition efficiency [32]. The data obtained from the present study indicates that the best inhibitor has the highest values of μ, while the lowest value of μ was calculated for the inhibitor that had the lowest inhibition efficiency.

Density functional theory (DFT)

DFT is based on solving the time-independent Schrödinger equation for the electrons of molecular systems as a function of the positions of the nuclei [33]. The premise behind the density functional theory is that the energy of a molecule can be determined from the electron density instead of a wavefunction [34].

The ionization potential (IP) and the electron affinity (EA) were calculated using the finite difference approximation as follows [35]:

$$IP = E_{(N-1)} - E_{(N)} \tag{8}$$

$$EA = E_{(N)} - E_{(N+!)}, \tag{9}$$

where $E_{(N-1)}$, $E_{(N)}$ and $E_{(N+1)}$ are the ground state energies of the systems with N−1, N and N+1 electrons, respectively. Calculated values of IE and EA are presented in Table 3. The results obtained indicate that the inhibition efficiencies of the

Table 6 Fukui and global softness indices for nucleophilic and electrophilic attacks on HDPPCARB, calculated from Mulliken (Löwdin) charges (STO-3G)

Atom	f^+ (|e|)	f^- (|e|)	S^+ (eV|e|)	S^- (eV|e|)
C1	−0.056 (−0.046)	−0.004 (−0.005)	−0.029 (−0.024)	−0.002 (−0.003)
C2	−0.088 (−0.095)	0.000 (0.000)	−0.045 (−0.049)	0.000 (0.000)
C3	−0.121 (−0.117)	0.005 (0.006)	−0.062 (−0.060)	0.003 (0.003)
C4	−0.018 (−0.014)	0.004 (0.005)	−0.009 (−0.007)	0.002 (0.003)
C5	−0.217 (−0.228)	−0.003 (−0.003)	−0.112 (−0.118)	−0.001 (−0.002)
C6	−0.153 (−0.157)	−0.005 (−0.006)	−0.079 (−0.081)	−0.002 (−0.003)
C7	−0.088 (−0.096)	−0.002 (−0.001)	−0.046 (−0.050)	−0.001 (0.000)
C8	−0.270 (−0.256)	−0.039 (−0.052)	−0.139 (−0.132)	−0.020 (−0.027)
C9	−0.333 (−0.321)	0.010 (0.012)	−0.172 (−0.166)	0.005 (0.006)
C10	−0.054 (−0.061)	0.004 (0.003)	−0.028 (−0.031)	0.002 (0.002)
C11	−0.055 (−0.102)	−0.002 (−0.002)	−0.029 (−0.052)	−0.001 (−0.001)
C12	−0.102 (−0.123)	−0.005 (−0.007)	−0.053 (−0.063)	−0.003 (−0.003)
C13	−0.203 (−0.210)	−0.004 (−0.005)	−0.105 (−0.109)	−0.002 (−0.002)
C14	−0.025 (−0.042)	−0.003 (−0.004)	−0.013 (−0.022)	−0.001 (−0.002)
O15	−0.016 (−0.015)	−0.009 (−0.009)	−0.008 (−0.008)	−0.005 (−0.005)
O16	−0.014 (−0.020)	−0.005 (−0.005)	−0.007 (−0.011)	−0.003 (−0.003)
N17	−0.125 (−0.153)	0.012 (0.022)	−0.064 (−0.079)	0.006 (0.011)
N18	0.002 (0.022)	−0.024 (−0.031)	0.001 (0.011)	−0.012 (−0.016)
C19	0.099 (0.048)	−0.012 (−0.008)	0.051 (0.025)	−0.006 (−0.004)
S20	0.710 (0.730)	−0.353 (−0.356)	0.366 (0.377)	−0.182 (−0.184)
N21	0.190 (0.191)	−0.022 (−0.024)	0.098 (0.099)	−0.011 (−0.012)
C22	0.122 (0.112)	−0.041 (−0.032)	0.063 (0.063)	−0.021 (−0.017)
C23	0.113 (0.129)	−0.025 (−0.026)	0.058 (0.066)	−0.013 (−0.014)
C24	−0.048 (−0.048)	−0.035 (−0.042)	−0.025 (−0.025)	−0.018 (−0.022)
C25	−0.019 (−0.026)	−0.026 (−0.026)	−0.010 (−0.013)	−0.013 (−0.013)
C26	0.195 (0.188)	−0.034 (−0.028)	0.101 (0.097)	−0.017 (−0.014)
C27	0.060 (0.070)	−0.105 (−0.143)	0.031 (0.036)	−0.054 (−0.074)

Table 7 Fukui and global softness indices for nucleophilic and electrophilic attacks on ODPPCARB, calculated from Mulliken (Löwdin) charges (STO-3G)

Atom	f^+ (|e|)	f^- (|e|)	S^+ (eV|e|)	S^- (eV|e|)
C1	1.208 (1.665)	2.130 (2.123)	0.338 (0.466)	0.596 (0.594)
C2	0.418 (0.568)	3.428 (3.322)	0.117 (0.159)	0.960 (0.930)
C3	−0.002 (0.008)	5.069 (4.975)	0.000 (0.000)	1.419 (1.393)
C4	0.036 (0.000)	6.152 (6.233)	0.010 (0.000)	1.723 (1.745)
C5	0.586 (1.195)	2.519 (3.197)	0.164 (0.334)	0.705 (0.895)
C6	7.403 (4.561)	−3.639 (−0.488)	2.073 (1.277)	−1.019 (−0.137)
C7	−2.877 (−3.273)	7.975 (7.932)	−0.806 (−0.916)	2.233 (2.221)
C8	−8.340 (−7.398)	6.900 (5.896)	−2.335 (−2.071)	1.932 (1.651)
C9	−0.716 (−1.152)	−1.022 (−0.711)	−0.200 (−0.322)	−0.286 (−0.199)
C10	−0.005 (−0.014)	−6.157 (−5.926)	−0.001 (−0.004)	−1.724 (−1.659)
C11	0.000 (0.000)	−4.162 (−4.183)	0.000 (0.000)	−1.165 (−1.171)
C12	0.000 (0.001)	−3.705 (−3.752)	0.000 (0.000)	−1.037 (−1.051)
C13	−0.015 (−0.042)	−2.008 (−2.054)	−0.004 (−0.012)	−0.562 (−0.575)
C14	−1.345 (−1.469)	0.958 (0.989)	−0.377 (−0.411)	0.268 (0.277)
N15	−1.301 (−1.218)	−5.337 (−4.566)	−0.364 (−0.341)	−1.494 (−1.278)
N16	0.004 (−0.003)	−8.036 (−7.978)	0.001 (−0.001)	−2.250 (−2.234)
C17	0.004 (0.000)	−8.027 (−7,961)	0.001 (0.000)	−2.248 (−2.229)
S18	0.000 (0.000)	−7.997 (−8.001)	0.000 (0.000)	−2.239 (−2.240)
N19	0.015 (0.008)	−6.408 (−6.255)	0.004 (0.002)	−1.794 (−1.751)
C20	0.007 (0.202)	0.957 (0.836)	0.002 (0.057)	0.268 (0.234)
C21	3.549 (3.112)	4.135 (3.687)	0.994 (0.871)	1.158 (1.032)
C22	3.741 (3.853)	1.074 (1.201)	1.048 (1.079)	0.301 (0.336)
C23	1.219 (3.554)	3.602 (0.899)	0.341 (0.995)	1.009 (1.009)
C24	1.351 (1.021)	4.852 (3.785)	0.378 (0.286)	1.359 (1.060)
C25	−1.189 (3.805)	3.805 (3.822)	−0.333 (−0.328)	1.065 (1.070)
O26	−7.983 (−7.724)	8.005 (7.997)	−2.235 (−2.163)	2.241 (2.239)

inhibitors increase with increasing ionization energy but decrease with decreasing electron affinity. This is because IP is directly related to E_{HOMO}, while EA is related to E_{LUMO}. Consequently, the trend for increasing inhibition efficiencies was similar to that obtained from the E_{HOMO} and E_{LUMO} data.

In DFT, the ground state energy $E(\rho)$ of an atom or molecule is usually expressed in terms of its electron density, $\rho(r)$. The first and second derivatives of $E(\rho)$ with respect to the number of electrons (N) define the chemical potential (σ) and the global hardness (η) of a molecule as follows [36]:

$$\sigma = (\delta E / \delta N)_{v(r)} \tag{10}$$

$$\eta = (\delta^2 E / \delta^2 N)_{v(r)}, \tag{11}$$

where $v(r)$ indicates that the differentiation is carried out under a constant external potential. Using the finite difference approximation, the global softness was evaluated as $S = 1/(IP−EA)$, while the global hardness is the inverse

of the global softness. Substituting for IP and EA (Eq. 8 and 9), the global softness becomes

$$S = 1 / [(E_{(N-1)} - E_{(N)}) - (E_{(N)} - E_{(N+!)})]. \tag{12}$$

Calculated values of S and η are also presented in Table 3. These parameters exhibit excellent correlation with the experimental inhibition efficiencies, as can be seen from the R^2 values depicted in Fig. 5.

The electron fraction transferred, δ, can be calculated using the following equation [37]:

$$\delta = (\phi_{Fe} - \phi_{inh}) / 2(\eta_{Fe} + \eta_{inh}) \tag{13}$$

where χ_{Fe} and χ_{inh} are the electronegativities of Fe and the inhibitor, respectively; $\chi = (IP + EA)/2$. η_{Fe} and η_{inh} are the global hardnesses of Fe and the inhibitor, respectively. In order to apply Eq. 11 to the present study, the theoretical values of $\chi_{Fe} = 7$ eV and $\eta_{Fe} = 0$ were used to compute the δ values for the various Hamiltonians. The calculated values of δ for the inhibitors are presented in Table 3. The results obtained indicate that the δ values correlate strongly with the experimental inhibition efficiencies (Fig. 5).

Fig. 6 HOMO and LUMO diagrams for the studied inhibitors
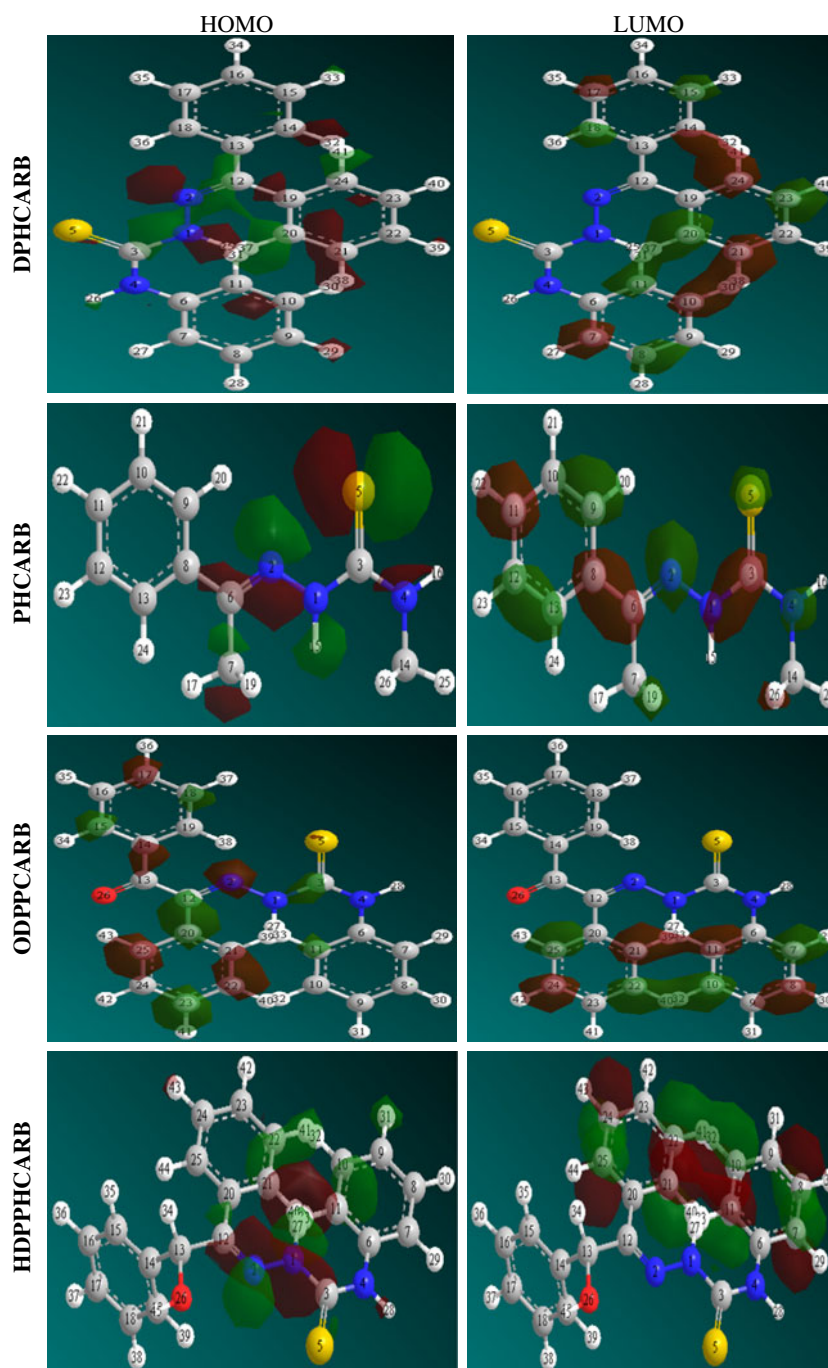
Local selectivity

The local selectivity of an inhibitor can be analyzed using the local Fukui and softness functions. These indices permit each part of a molecule to be distinguished on the basis of its chemical behavior due to the presence of different substituent functional groups. The Fukui function derives from the fact that if an electron δ is transferred to an N-electron molecule, it will tend to distribute so as to minimize the energy of the resulting $(N + \delta)$-electron system. The resulting changes in electron density are given by the nucleophilic (f^+) and electrophilic (f^-) Fukui functions, which can be calculated using the finite difference approximation as follows [37]:

$$f^+ = (\delta\rho(r)/\delta N)_v^+ = q_{(N+1)} - q_{(N)} \tag{14}$$

$$f^+ = (\delta\rho(r)/\delta N)_v^- = q_{(N)} - q_{(N-1)}, \tag{15}$$

Table 8 Theoretical inhibition efficiencies (IE$_{Theor}$) of the studied compounds

Inhibitor	C (M)	Inhibition efficiency (%)				
		PM6	PM3	AM1	RM1	MNDO
PHCARB	1×10^{-4}	98.92	99.93	99.11	99.20	99.33
	2×10^{-4}	99.46	99.96	99.55	99.60	99.66
	3×10^{-4}	99.64	99.98	99.7	99.73	99.77
	4×10^{-4}	99.73	99.98	99.78	99.80	99.83
	5×10^{-4}	99.78	99.99	99.82	99.84	99.86
DPHCARB	1×10^{-4}	99.18	99.92	99.30	99.36	99.44
	2×10^{-4}	99.59	99.97	99.65	99.68	99.72
	3×10^{-4}	99.73	99.97	99.77	99.79	99.81
	4×10^{-4}	99.79	99.98	99.83	99.84	99.86
	5×10^{-4}	99.84	99.99	99.86	99.87	99.89
HDPPCARB	1×10^{-4}	99.14	99.93	99.27	99.34	99.42
	2×10^{-4}	99.57	99.96	99.63	99.67	99.71
	3×10^{-4}	99.71	99.96	99.76	99.78	99.81
	4×10^{-4}	99.78	99.98	99.82	99.83	99.85
	5×10^{-4}	99.83	99.99	99.85	99.87	99.88
ODPPCARB	1×10^{-4}	79.09	79.93	79.23	79.31	79.40
	2×10^{-4}	79.54	79.95	79.62	79.65	79.69
	3×10^{-4}	79.69	79.98	79.74	79.77	79.8
	4×10^{-4}	79.77	79.98	79.81	79.82	79.85
	5×10^{-4}	79.82	79.99	79.84	79.86	79.88

where ρ, $q_{(N+1)}$, $q_{(N)}$, and $q_{(N-1)}$ are the electron density and the Mulliken charges on the atom with N+1, N and N−1 electrons, respectively. Calculated values of f^+ and f^- for the studied inhibitors are presented in Tables 4, 5, 6 and 7. It is expected that the site for nucleophilic attack will be the site where the value of f^+ is maximum, while the site for electrophilic attack is controlled by the value of f^-. If it is assumed that the protonated forms of the inhibitor molecules have a net positive charge, it can be deduced that the sites for nucleophilic attack are the nitrogen atom N10, the sulfur atom S20, and the carbon atoms C6 and C12 for PHCARB, HDPPCARB, ODPPCARB, and DPHCARB, respectively, while the sites for electrophilic attack are the nitrogen atoms N9 and N17, the oxygen atom O26, and the nitrogen atom N2, respectively.

The HOMO and LUMO orbitals of PHCARB, HDPPCARB, ODPPCARB, and DPHCARB are presented in Fig. 6. The figure supports the information obtained from the Fukui functions.

The local softness, S, of an atom is the product of the condensed Fukui function (f) and the global softness (S), as expressed by Eqs. 16 and 17 [38]:

$$S^+ = (f^+)S \tag{16}$$

$$S^- = (f^-)S. \tag{17}$$

The local softness contains information similar to that obtained from the condensed Fukui function, plus additional information about the total molecular softness, which is related to the global reactivity with respect to a reaction partner. The sites for electrophilic and nucleophilic attacks found from the global function indices were similar to those obtained from the Fukui functions. Similar information was also obtained from the relative nucleophilicity and the relative electrophilicity. The relative nucleophilicity and electrophilicity are defined as (S^+/S^-) and (S^-/S^+), respectively. These functions have been successfully applied to predict reactivity sequences of carbonyl compounds with respect to nucleophilic attack. It was observed that the atoms with the highest values of relative nucleophilicity and electrophilicity are similar to those obtained for the Fukui and global softness functions (results not presented).

Quantitative structure–activity relation (QSAR) study

Attempts were made to correlate some quantum chemical parameters (calculated for the different models) with experimental corrosion inhibition efficiencies using multiple linear regressions. The tests reveal that there is no simple or direct linear relationship between inhibition efficiency and the calculated quantum chemical parameters. This indicates that the inhibition
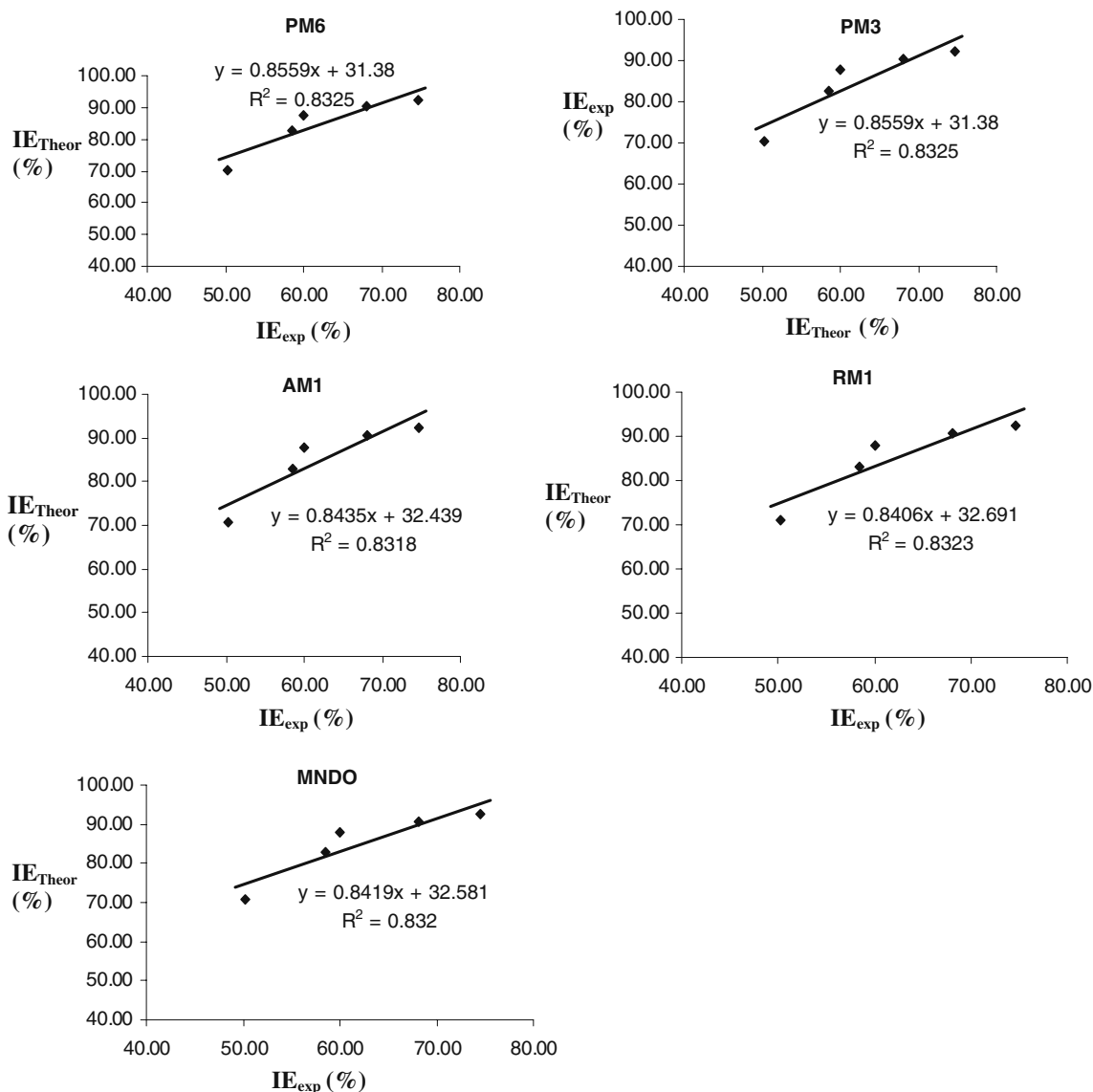
Fig. 7 Variation of the theoretical inhibition efficiency with the experimental inhibition efficiency for various concentrations of PHCARB

efficiencies of the inhibitors depend on composite functions that cannot be adequately expressed by linear models. The linear model approximates the corrosion inhibition efficiency (E_{cal} in %) with quantum chemical parameters as follows [39]:

$$E_{cal} = Ax_jC_i + B, \tag{18}$$

where A and B are constants obtained by regression analysis; x_j is a quantum chemical index characteristic of molecule j; and C_i denotes the concentration of the inhibitor. This linear approach was found to be unsatisfactory for deriving correlations between the results obtained in this investigation. Therefore, the nonlinear model proposed by Lukovits and coworkers for studying

the interaction of corrosion inhibitors with a metal surface in an acidic medium was used [40]:

$$IE_{Theor} = \frac{(AE_{HOMO} + BE_{LUMO} + CE_{L-H} + D\mu - E*IP + F)C_{inh}}{(1 + (AE_{HOMO} + BE_{LUMO} + CE_{L-H} + D\mu - E*IP + F)C_{inh}}, \tag{19}$$

where A, B, C, D and E are regression coefficients. Using the nonlinear equation (Eq. 19), Eqs. 20, 21, 22, 23 and 24 were obtained for the PM6, PM3, AM1, RM1, and MNDO Hamiltonians, respectively. The corresponding correlation coefficients (r) between the theoretical (IE_{Theor}) and experimental (IE_{exp}) inhibition efficiencies were 0.9124, 0.9124, 0.9121, 0.9122, and 0.9122, respectively.
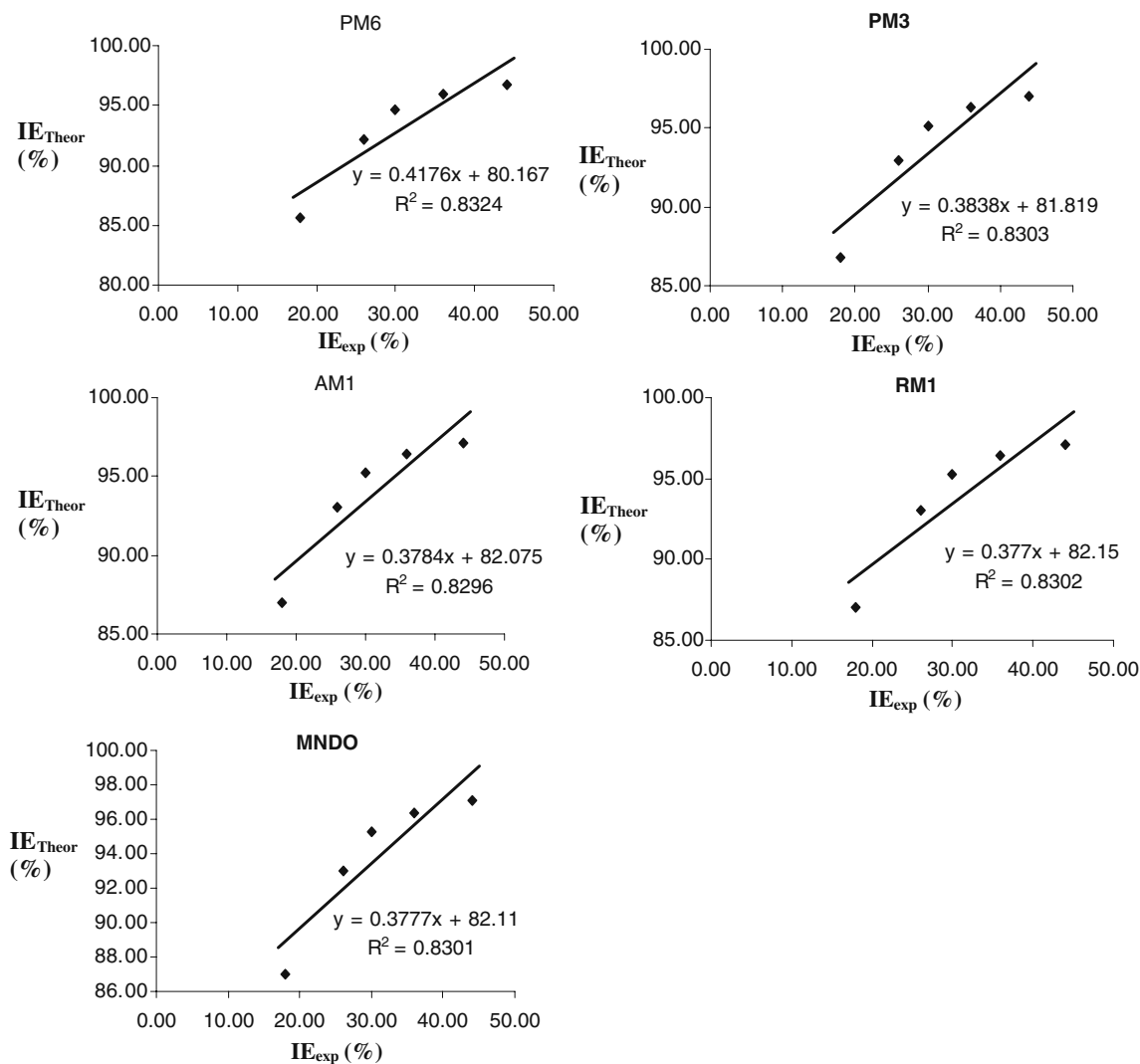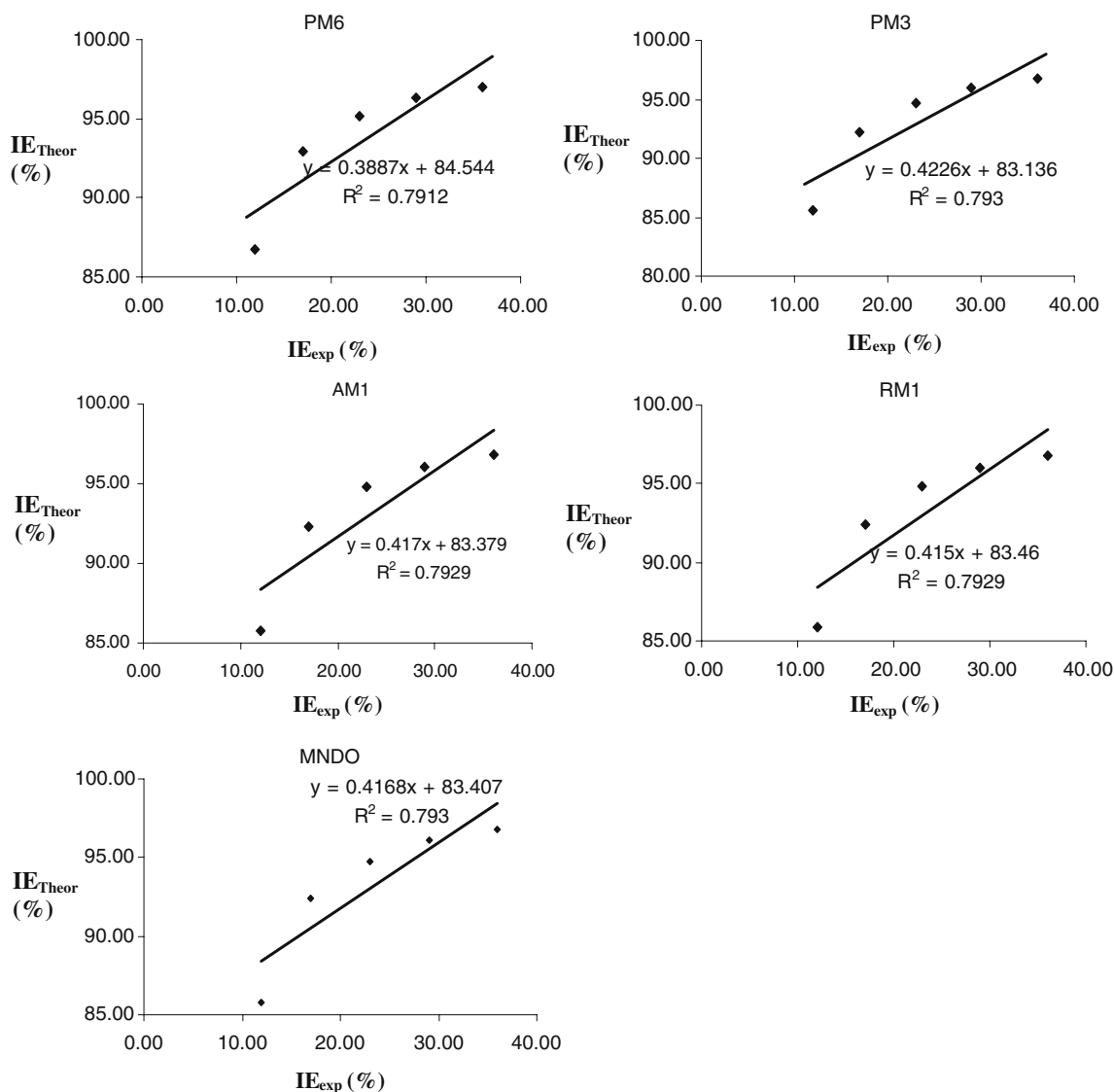
Fig. 8 Variation of the theoretical inhibition efficiency with the experimental inhibition efficiency for various concentrations of HDPPCARB

$$IE_{Theor} = \frac{(1.0176E_{HOMO} + 0.9743_{LUMO} + 1.0351*\Delta E + CosA + CosV + 428.6731)C}{(1 + (1.0176E_{HOMO} + 0.9743E_{LUMO} + 1.0351\Delta E + CosA + CosV + 428.6731)C} \qquad (20)$$

$$IE_{Theor} = \frac{(1.042E_{HOMO} + 0.9418E_{LUMO} + \Delta E + CosA + 1.1033CosV + 13690)C}{(1 + (1.042E_{HOMO} + 0.9418E_{LUMO} + \Delta E + CosA + 1.1033CosV + 13690)C)} \qquad (21)$$

$$IE_{Theor} = \frac{(1.0172E_{HOMO} + 0.9748E_{LUMO} + \Delta E + 1.1402CosA + CosV + 594.4694)C}{(1 + (1.0172E_{HOMO} + 0.9748E_{LUMO} + \Delta E + 1.1402CosA + CosV + 594.4694)C)} \qquad (22)$$

Fig. 9 Variation of the theoretical inhibition efficiency with the experimental inhibition efficiency for various concentrations of ODPPCARB

$$IE_{Theor} = \frac{(1.0199E_{HOMO} + 0.9712E_{LUMO} + \Delta E + 1.1194CosA + CosV + 735.6791)C}{(1 + (1.0199E_{HOMO} + 0.9712E_{LUMO} + \Delta E + 1.1194CosA + CosV + 735.6791)C)} \quad (23)$$

$$IE_{Theor} = \frac{(1.0225E_{HOMO} + 0.9676E_{LUMO} + \Delta E + 1.0978CosA + CosV + 965.079)C}{(1 + (1.0225E_{HOMO} + 0.9676E_{LUMO} + \Delta E + 1.0978CosA + CosV + 965.079)C} \quad (24)$$

Theoretical inhibition efficiencies calculated from Eqs. 20–24 are presented in Table 8, while Figs. 7, 8, 9 and 10 show plots of the variation in theoretical inhibition efficiency versus the experimental inhibition efficiency for PHCARB, HDPPCARB, ODPPCARB, and

DPHCARB, respectively. From the figures, it is evident that the degree of linearity (R^2) of the plots are very close to unity, indicating that there is a strong agreement between the theoretical and experimental inhibition efficiencies. It was also observed that the R^2 values
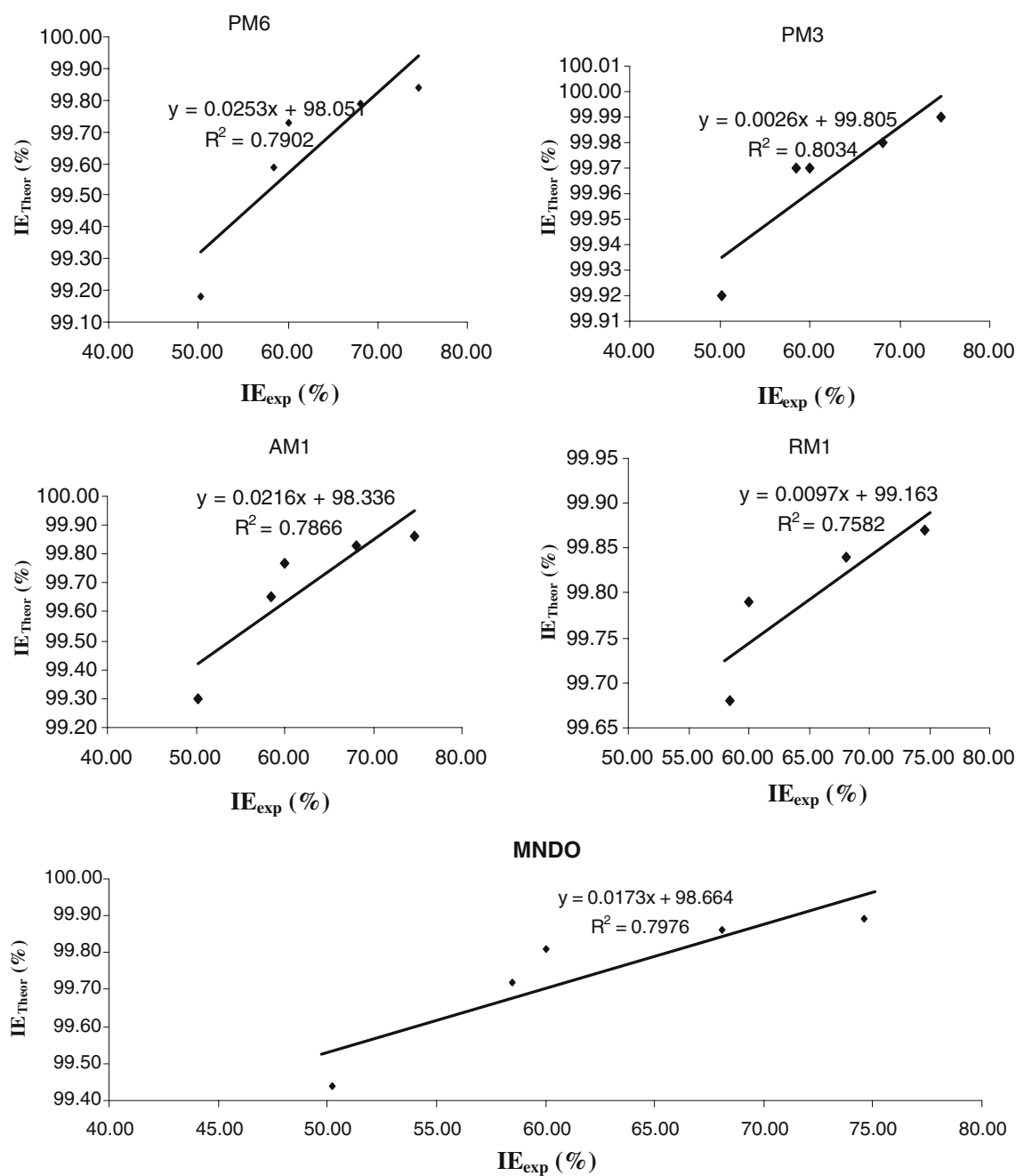
Fig. 10 Variation of the theoretical inhibition efficiency with the experimental inhibition efficiency for various concentrations of DPHCARB

obtained for different Hamiltonians did not differ significantly from each other. For PHCARB, HDPPCARB, ODPPCARB, and DPHCARB, the values of R^2 were approximately equal to 0.84, 0.83, 0.79, and 0.80, respectively. These values are above average, indicating that any of these Hamiltonians can be used to model the inhibition behaviors of the studied compounds, or compounds that are structurally related to the studied compounds.

Conclusions

PHCARB, HDPPCARB, ODPPCARB, and DPHCARB are good adsorption inhibitors of the corrosion of mild steel in HCl. The adsorption of the inhibitors onto a mild steel surface is spontaneous and is consistent with the Langmuir adsorption model. Quantum chemical parameters, DFT, and QSAR can be used to model the inhibition potentials of PHCARB, HDPPCARB, ODPPCARB, DPHCARB, and

375

compounds that are structurally related to them. The PM6 Hamiltonian gives the best model for predicting the inhibition potentials of the studied carbozones.

References

1. Noor EA (2009) Potential of aqueous extract of *Hibiscus sabdariffa* leaves for inhibiting the corrosion of aluminium in alkaline solutions. J Appl Electrochem 39:1465–1475
2. Eddy NO, Odoemelam SA, Odiongenyi (2009) Joint effect of halides and ethanol extract of *Lasianthera Africana* on the inhibition of the corrosion of mild steel in H_2SO_4. J Appl Electrochem 39:849–857
3. Eddy NO, Ibok UJ, Ebenso EE (2009) Adsorption, synergistic inhibitive effect and quantum chemical studies on ampicillin and halides for the corrosion of mild steel. J Appl Electrochem 40:445–456
4. Keleş H, Keleş M, Dehri I, Serindağ O (2008) The inhibitive effect of 6-amino-*m*-cresol and its Schiff base on the corrosion of mild steel in 0.5 M HCl medium. Mat Chem Phys 112:173–179
5. Achary G, Sachin HP, Naik YA, Venkatesha TV (2008) The corrosion inhibition of mild steel by 3-formyl-8-hydroxy quinoline in hydrochloric acid medium. Mat Chem Phys 107:44–50
6. Quraishi MA, Ahamad I, Singh AK, Shukla SK, Lal B, Singh V (2008) N-(Piperidinomethyl)-3-[(pyridylidene)amino]isatin: a new and effective acid corrosion inhibitor for mild steel. Mat Chem Phys 112:1035–1039
7. Emregul KC, Hayvali M (2006) Studies on the effect of a newly synthesized Schiff base compound from phenazone and vanillin on the corrosion of steel in 2 M HCl. Corros Sci 48:797–812
8. Eddy NO, Ebenso EE (2009) Quantum chemical studies on the inhibition potentials of some penicillin compounds for the corrosion of mild steel in 0.1 M HCl. J Mol Model. doi:10.1007/S00894-0090635-6
9. Eddy NO, Odoemelam SA (2009) Inhibition of the corrosion of mild steel in H_2SO_4 by ethanol extract of *Aloe vera*. Pigment Resin Technol 38:111–115
10. Eddy NO, Odoemelam SA, Odiongenyi AO (2009) Inhibitive, adsorption and synergistic studies on ethanol extract of *Gnetum africana* as green corrosion inhibitor for mild steel in H_2SO_4. Green Chem Lett Rev 2:111–119
11. Eddy NO, Ekwumengbo PA, Mamza PAP (2009) Ethanol extract of *Terminalia catappa* as a green inhibitor for the corrosion of mild steel in H_2SO_4. Green Chem Lett Rev 2:223–231
12. Mohana KN, Badiea AM (2009) Effect of sodium nitrite–borax blend on the corrosion rate of low carbon steel in industrial water medium. Corros Sci 50:2939–2947
13. Eddy NO, Ibok UJ, Ebenso EE, El Nemr A, El Ashry H (2009) Quantum chemical study of the inhibition of the corrosion of mild steel in H_2SO_4 by some antibiotics. J Mol Model 15:1085–1092
14. Bentiss F, Bouanis M, Mernari B, Traisnel M, Vezin H, Lagrene´e M (2007) Understanding the adsorption of 4H-1,2,4-triazole derivatives on mild steel surface in molar hydrochloric acid. Appl Surf Sci 253:3696–3704
15. Achary G, Sachin HP, Naik YA, Venkatesha TV (2008) The corrosion inhibition of mild steel by 3-formyl-8-hydroxy quinoline in hydrochloric acid medium. Mat Chem Phys 107 (07):44–50

16. Sahin M, Gece G, Karci F, Bilgic S (2008) Experimental and theoretical study of the effect of some heterocyclic compounds on the corrosion of low carbon steel in 35% NaCl medium. J Appl Electrochem 38:809–815
17. Fang J, Lie J (2002) Quantum chemistry study of the relationship between molecular structure and corrosion inhibition efficiency of amides. J Mol Struct (THEOCHEM) 593:179–185
18. Gomez B, Likhanova NV, Dominguez-Aguliar MA, Martinez-Paulou P (2006) Quantum chemical study of the inhibitive properties of 2-pyridyl-azoles. J Phys Chem B 110:8928–8934
19. Eddy NO (2010) Theoretical study on some amino acids and their potential activity as corrosion inhibitors for mild steel in HCl. Mol Simul 40:445–456
20. Ashassi-Sorkhabi H, Shaabani B, Seifzadeh D (2005) Effect of some pyrimidine schiff bases on the corrosion of mild steel in HCl solution. Electrochim Acta 50:3446–3452
21. Singh P, Bhrara K, Singh G (2008) Adsorption and kinetic studies of L-leucine as an inhibitor on mild steel in acidic media. Appl Surf Sci 254:5927–5935
22. Eddy NO, Mamza PAP (2009) Inhibitive and adsorption properties of ethanol extract of seeds and leaves of *Azardirachta indica* on the corrosion of mild steel in H_2SO_4. Port Electrochim Acta 27:443–456
23. Ebenso EE, Eddy NO, Odiongenyi AO (2008) Corrosion inhibitive properties and adsorption behaviour of ethanol extract of *Piper guinensis* as a green corrosion inhibitor for mild steel in H_2SO_4. Afr J Pure Appl Chem 4:107–115
24. Odoemelam SA, Ogoko EC, Ita BI, Eddy NO (2009) Inhibition of the corrosion of zinc in H_2SO_4 By 9-deoxy-9a-aza-9a-methyl-9a-homoerythromycin A (azithromycin). Port Electrochim Acta 27:57–68
25. Odiongenyi AO, Odoemelam SA, Eddy NO (2009) Corrosion inhibition and adsorption properties of ethanol extract of *Vernonia amygdalina* for the corrosion of mild steel in H_2SO_4. Port Electrochim Acta 27:33–45
26. Keleş H, Keleş M, Dehri I, Serinda O (2008) The inhibitive effect of 6-amino-*m*-cresol and its Schiff base on the corrosion of mild steel in 0.5 M HCl medium. Mat Chem Phys 112:173–179
27. Yurt A, Bereket G, Ogretir C (2005) Quantum chemical studies on inhibition effect of amino acids and hydroxy carboxylic acids on pitting corrosion of aluminium alloy 7075 in NaCl solution. J Mol Struct 725:215–221
28. Khaled KF, Babić-Samardžija K (2005) Theoretical study of the structural effects of polymethylene amines on corrosion inhibition of iron in acid solutions. Electrochim Acta 50:2515–2520
29. Bentiss F, Lebrini M, Lagrenée M, Traisnel M, Elfarouk A, Vezin H (2007) The influence of some new 2,5-disubstituted 1,3,4-thiadiazoles on the corrosion behaviour of mild steel in 1 M HCl solution: AC impedance study and theoretical approach. Electrochim Acta 52:6865–6872
30. Arslan T, Kandemirli F, Ebenso EE, Love I, Alemu H (2009) Quantum chemical studies on the corrosion inhibition of some sulphonamides on mild steel in acidic medium. Corros Sci 51:35–47
31. El Ashry HE, El Nemr A, Esawy SA, Ragab S (2006) Corrosion inhibitors. Part II: Quantum chemical studies on the corrosion inhibitions of steel in acidic medium by some triazole oxadiazole and thiadiazole derivatives. Electrochim Acta 51:3957–3968
32. Xia S, Qiu M, Yu L, Liu F, Zhao H (2008) Molecular dynamics and density functional theory study on relationship between structure of imidazoline derivatives and inhibition performance. Corros Sci 50:2021–2029

33. Young DC (2001) Computational chemistry, a practical guide for applying techniques to real world problems. Wiley, New York

34. Stayanov SR, Kral P (2006) Metallopyrrole-capped carbon nanocones. J Phys Chem B 110:21480–21486

35. Stoyanov SR, Gusarov S, Kuznick SM, Kovalenko A (2008) Theoretical modelling of zeolite nanoparticle surface activity for heavy oil upgrading. J Phys Chem C 112:6794–6810

36. Wang H, Wang X, Wang H, Wang L, Liu A (2007) DFT study of new bipyrazole derivatives and their potential activity as corrosion inhibitors. J Mol Model 13:147–153

37. Fukui K (1975) Theory of orientation and stereo selection. Springer, New York

38. Gokhan G (2008) The use of quantum chemical methods in corrosion inhibitor studies. Corros Sci 50:2961–2992

39. El Ashry HE, El Nemr A, Esawy SA, Ragab S (2006) Corrosion inhibitors. Part IV: Quantum chemical studies on the corrosion inhibition of steel in acidic medium by some aniline derivatives. J Phys Chem 1:41–55

40. Lukovitis I, Shaban A, Kalman E (2003) Corrosion inhibitors: quantitative structure activity relationships. Russ J Electrochem 39:177–181